The Designing of an Air-gap Type FBAR Filter using Leach Equivalent Model

Hyung-Wook Choi[a], Joong-Yeon Jung, Seung-Kyu Lee, Yong-Seo Park, and Kyung-Hwan Kim
Department of Electrical and Information Engineering, Kyungwon University, San 65 Bokjeong-dong, Sujeong-gu, Seongnam-si, Gyeonggi 461-701, Korea

Hyun-Yong Shin
Department of Electronics and Information Communication Engineering, Namseoul University, Seonghwan-eup, Cheonahn-si, Choongnam 330-707, Korea

[a]E-mail : chw@kyungwon.ac.kr

(Received March 21 2006, Accepted August 10 2006)

An air-gap type FBAR was designed using Leach equivalent model for analyzing a vertical structure of the FBAR. For the top electrode, Pt, and the bottom electrode, Au, of 1.2 ㎛ thickness and the piezoelectric of 0.8 ㎛ thickness, the resonance and anti-resonance occurred at 2.401 GHz and 2.460 GHz, respectively. S_{11} was increased and S_{21} was decreased as the resonance area of FBAR was widened. We observed the characteristics of insertion loss, bandwidth and out-of-band rejection of ladder-type FBAR BPF by changing resonance areas of series and shunt resonators and by adding stages. As the resonance area of series resonator was increased, insertion loss was improved but out-of-band rejection was degraded. And as the resonance area of shunt resonator was increased, insertion loss was degraded a little but out-of-band rejection was improved even without adding stages. We, also, changed the shape of the resonance area from square shape to rectangle shape to examine the effects of the resonator shape on the characteristics of the BPF. The best performances were observed when the sizes of series and shunt resonator are 150 ㎛×150 ㎛ and 5 ㎛×50 ㎛, respectively. Out-of-band rejection was improved about 10 dB and bandwidth was broadened from 30 MHz to 100 MHz utilizing inductor tuning on 2×2 and 4×2 ladder-type BPFs.

Keywords : FBAR, Leach equivalent model, BPF, Resonance

1. INTRODUCTION

Recently, demands on higher data rate wireless local area network (WLAN) systems using orthogonal-frequency-division multiplexing (OFDM) communication system in 2.4 GHz band are increasing. In order to implement equipments of 2.4 GHz OFDM system, radio frequency (RF) band-pass filter (BPF) is one of the important devices. The requirements of the RF BPF are wide bandwidth, low insertion loss, flat group-delay, small-size, easy fabrication and low fabrication cost. For example, center frequency of 2.4 GHz and bandwidth of 100 MHz are required for IEEE802.11a system in Japan[1-3].

For conventional wireless system such as a cellular phone, surface-acoustic wave (SAW) filter is usually used for RF band-pass filter. However, it is difficult to fabricate interdigital transducers (IDTs) for 2.4 GHz SAW filter. Furthermore, insertion loss was increasing, because the propagation loss of SAW proportionally increases with square of increasing operation frequency. Therefore, a new type of filter is required to solve theses problems and to integrated with active and passive elements for on-chip fabrication. Piezoelectric thin film bulk acoustic resonator (FBAR) satisfies these requirements. And the fabrication of RF BPF based on FBAR is relatively simple. Because the substrate of FBAR is silicon (Si), FBAR can be made by monolithic microwave integrated circuit (MMIC). FBAR is economically attractive because it has advantages of small size, low cost by mass production and compatibility with semiconductor process. FBAR filter is suitable for 2.4 GHz RF band-pass filter. Aluminum nitride (AlN) and zinc oxide (ZnO) are the commonly used piezoelectric materials for FBAR fabrication. However, AlN is more suitable for the application to RF

filter at high frequencies[4-6]. In order to fabricate wideband FBAR filter, high Q-factor of FBAR is required, and K_t^2 of AlN film decides the Q-factor of FBAR[7].

The purpose of this study is to investigate the relationship between the area of resonance and the center frequency by analyzing the characteristics of 2-port resonator. This was done by ideal design using Leach model which is the modified Mason model and equivalent circuit for the application of resonator bandpass filter at high-frequency band. The changes in bandwidth, insertion loss, and out-of-band rejection as function of the number of resonators and the areas of resonators were, also, observed using FBAR ladder-type BPF. An optimization of BPF based on the resonator structure using inductor tuning to improve the characteristics of bandwidth and out-of-rejection of piezoelectric FBAR were attempted.

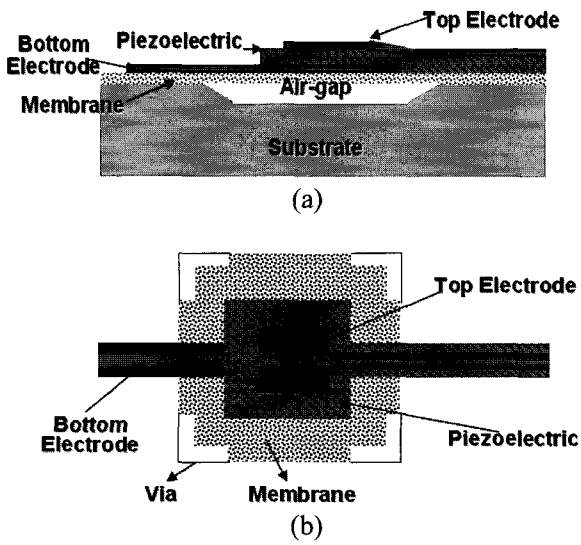

Fig. 1. Structure of air-gap type FBAR; (a) cross-sectional view and (b) top view.

2. DESIGN OF FBAR AND BPF

2.1 Design of air-gap type FBAR

It is possible to build FBARs with various features, such as air-gap types, back-etched types, solidly mounted types, and so on. An air-gap type FBAR has an advantage in fabrication compared to back etched or solidly mounted types. The latter two types have complex fabrication procedures, because they must have the substrate etched and several layers stacked up under the electrode to form a Bragg-type reflector. Figure 1 shows the cross sectional view and top view of the air-gap type FBAR used in this study. Aluminum nitride is sandwiched between the top and bottom electrodes, and a very thin air gap is placed under the membrane to avoid the over-mode phenomenon due to the silicon substrate loading effect.

2.2 Leach equivalent circuit model for an air-gap type FBAR

Mason's model[8,9] is one of the most widely used for the analysis of piezoelectric materials; however, it contains a transformer and a negative capacitance, which impose difficulties in the development of computer-aided design. Leach[10] developed previous work further and devised SPICE models with controlled sources to overcome the disadvantages of a transformer and a negative capacitance. Leach's circuits are modeled for both the thickness-mode and the side electrode bar piezoelectric mode. Only the thickness-mode piezoelectric structure is considered here, because the side-electrode bar mode is negligible for the small area size of the FBAR.

Figure 2 shows the Leach equivalent circuit model for air-gap type FBAR proposed in this research. Transmission lines are used to characterize the top and bottom electrodes, membrane, air-gap and silicon substrate. Transmission-line model parameters are acoustic impedance Z, electrical length E in degrees, and resonance frequency of piezoelectric material F, which decides the electrical length E. These parameters were calculated using the following equations.

$$Z = \rho v_a A, \quad E = \frac{360dF}{v_a}, \quad F = \frac{v_a\sqrt{\pi^2 - 8k_t^2}}{2\pi d_p} \tag{1}$$

They are given as where ρ is the density of the material, V_a is the acoustic velocity of the material, A is the area, d is the thickness of the material, K_t^2 is the electromechanical coupling constant and d_p is the thickness of the piezoelectric material. One voltage-controlled voltage source (VCVS) and two current controlled current sources (CCCS) are used to substitute for the transformer and the negative capacitance in Mason's model. Each CCCS has the gain of $G_1 = hC_0$ and $G_2 = h$, where h is obtained from material stiffness constant. C_0 is the electrical capacitance between two electrodes and depends on three parameters: the dielectric constant of piezoelectric material, area of the FBAR, and distance between the electrodes *dp*. R_n and C_n are included to prevent the node from being a floating node. The material parameters used to obtain the transmission-line model parameters are summarized in Table 1.

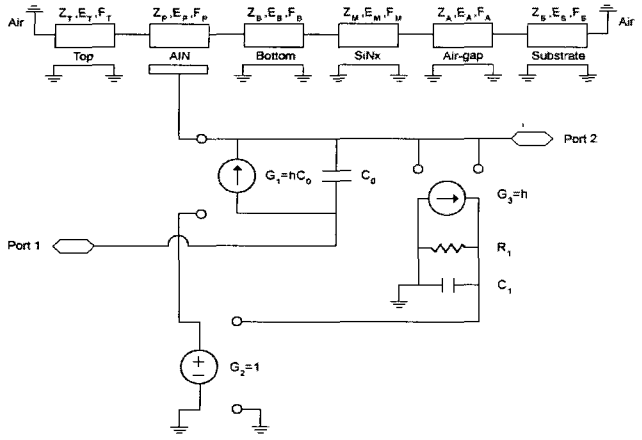

Fig. 2. Leach equivalent circuit model for air-gap type FBAR in ADS.

The characteristics of resonance and anti-resonance are evaluated by changing the thicknesses of AlN, top and bottom electrode, and the area of resonance. The thicknesses of the AlN, top electrode, bottom electrode, membrane, air gap, and substrate for FBAR with resonance frequency of 2.4 GHz are 0.8, 0.12, 0.12, 0.2, 1.5, 500 ㎛, respectively. The resonance area of the FBAR was 150 ㎛ x 150 ㎛. These are summarized in Table 2.

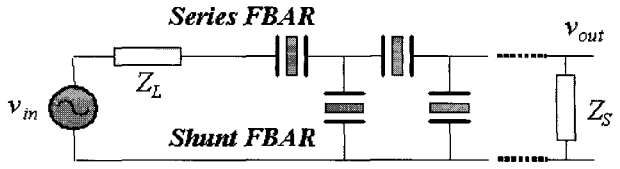

Fig. 3. Equivalent circuit of an FBAR ladder-type filter.

2.3 FBAR ladder-type BPF

There have been several approaches to constructing FBAR filters[11]. In this study, we have investigated the ladder filter configuration, which uses series and shunt FBARs. To design such filters, we have used the equivalent-circuit representation previously described for AlN FBAR. Figure 3 shows the equivalent circuit of a FBAR ladder-type filter consisting of series and shunt FBARs. The FBAR ladder-type filter can be expressed as M×N, where M is the number of series FBARs and N is the number of shunt FBARs connected. The insertion loss of a ladder-type filter is determined not only by the value of each FBAR, but also by the accuracy with which the resonant frequencies of series and shunt FBARs can be modeled and achieved experimentally. The smallest insertion loss is obtained when the parallel resonance frequency of the shunt FBAR is adjusted to be equal to series resonance frequency of the series FBAR. This can be achieved by adjusting the thickness of any of the layers within the shunt FBARs. The out-of-band rejection is determined by the S_{11} of the series FBARs

Table 1. Material parameters used in the model.

Materials	Density (Kg/m^3)	Dielectric Constant	Acoustic Velocity (m/s)	Acoustic Impedance ($10^{-6}kg/m^2s$)	Electromechanical Coupling Factor, K_t^2	Δ f/fr
AlN	3,370	10.4	10,400	37	0.03	1
Pt	21,300		3,250	69.9		
SiNx	3,100	4.5	3,100	20.8		
Air	12	1	330	$4e^{-3}$		
Au	19,320		3,240	62.6		
Si	2,332	11.9	8,430	19.7		

Table 2. Thickness of each material used for 2.4 GHz FBAR design.

Material	Thickness (㎛)
Top - Pt	0.12
Piezoelectric-AlN	0.8
Bottom -Au	0.12
Membrane – Si_3N_4	0.2
Air-gap	1.5
Substrate-Si	500

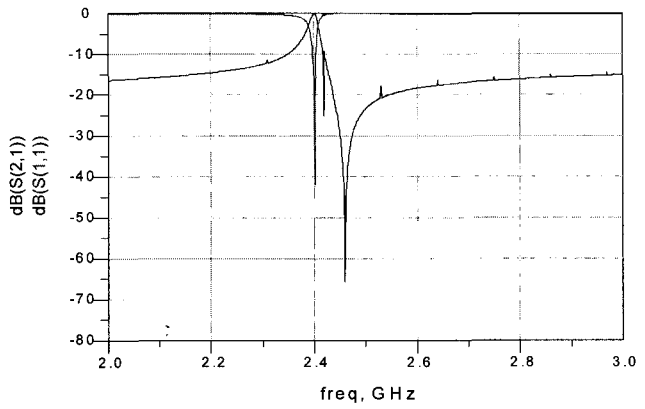

Fig. 4. Simulation result of FBAR with resonance area 30×30 ㎛ 2.

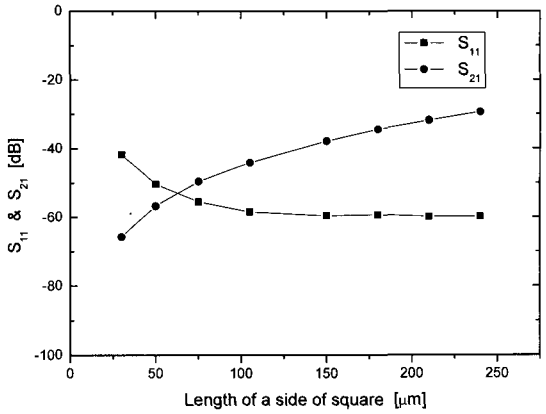

Fig. 5. S11 and S21 of FBAR as a function of resonance area.

and the S_{21} of the shunt FBARs. Also, it is apparent that the smaller area for the series FBARs and the larger area for the shunt FBARs will help increase the out-of-band rejection. Therefore, the areas of series and shunt FBARs in ladder-type FBAR filter are the one of design variables considered.

3. SIMULATION RESULTS

3.1 Simulation results of FBAR

The characteristics of FBAR with different resonance areas were simulated using the thickness of electrodes and AlN presented in Table 2. Figure 4 shows the typical frequency responses obtained from the designed FBARs. Figure 5 shows the simulation results as a function of resonance area of FBAR, in true square shape, changing from 30 ㎛×30 ㎛ to 240 ㎛×240 ㎛. The resonance frequency and anti-resonance frequency of the simulated FBARs are 2.401 GHz and 2.460 GHz, respectively, regardless of the resonance areas of FBARs. This indicated that the resonance frequency and anti-resonance frequency of FBAR were not a function of resonance area of the FBAR. As the resonance area was increased, return loss (S_{11}) at resonance frequency was increased and insertion loss (S_{21}) at anti-resonance frequency was decreased at resonance frequency. In general, S_{11} and S_{21} of piezoelectric resonator show the opposite tendency with resonance area increases if there is no influence from parasitic components. As a results, changes of these resonance characteristics confirmed numerically that very large decrease of Q value and decrease of K_t^2 value were due to parasitic capacitance.

While changing resonance area ratio from 0.1 to 0.5, the characteristics of FBAR were simulated to examine the resonance area effects on the performance of the FBAR. The resonance area changed by reducing the length of one side of square while maintain the length of the other side of square. Figure 6 shows the simulation results of FBARs in accordance with resonance area ratios. For FBAR with resonance area of 30 ㎛ × 30 ㎛, the return loss (S_{11}) was decreased by 21.921 dB from 41.828 dB to 19.287 dB when the resonance area was reduced to one tenth. S_{11} of FBAR with resonance area of 240 ㎛ × 240 ㎛ fell off by 3.75 dB from 59.955 dB to 56.205 dB when the resonance area was reduced to 1/10. However, insertion loss (S_{21}) was almost unchanged with resonance area reduction. From the results, we could find that the smaller the resonance area is, the larger the change of S_{11} is and S_{21} is affected a little by the resonance area variations. When resonance area of FBAR was increased, S_{21} and S_{11} showed opposite tendency if there is no effect from parasitic components.

3.2 Simulation results of FBAR filter

Using the above results, we estimated the characteristics of ladder-type FBAR filters prior to designing BPFs. The loss was induced from electrical resistance and parasitic components regardless of the connecting type of FBARs. Insertion loss and out-of band rejection characteristics of 1×1, 2×1, 2×2, 3×3, and 4×2 FBAR filters with different resonance areas were observed. S-parameters at 2.2 GHz~3 GHz band were simulated using ADS and the results were presented in Table 3.

As the number of resonator was increased, the insertion loss of 1×1 filter was increased about 6 times than that of 3×3 filter, which was from 3.546 dB to 19.106 dB with the bandwidth between 28 MHz and 31 MHz. The insertion loss was improved from 19.106 dB

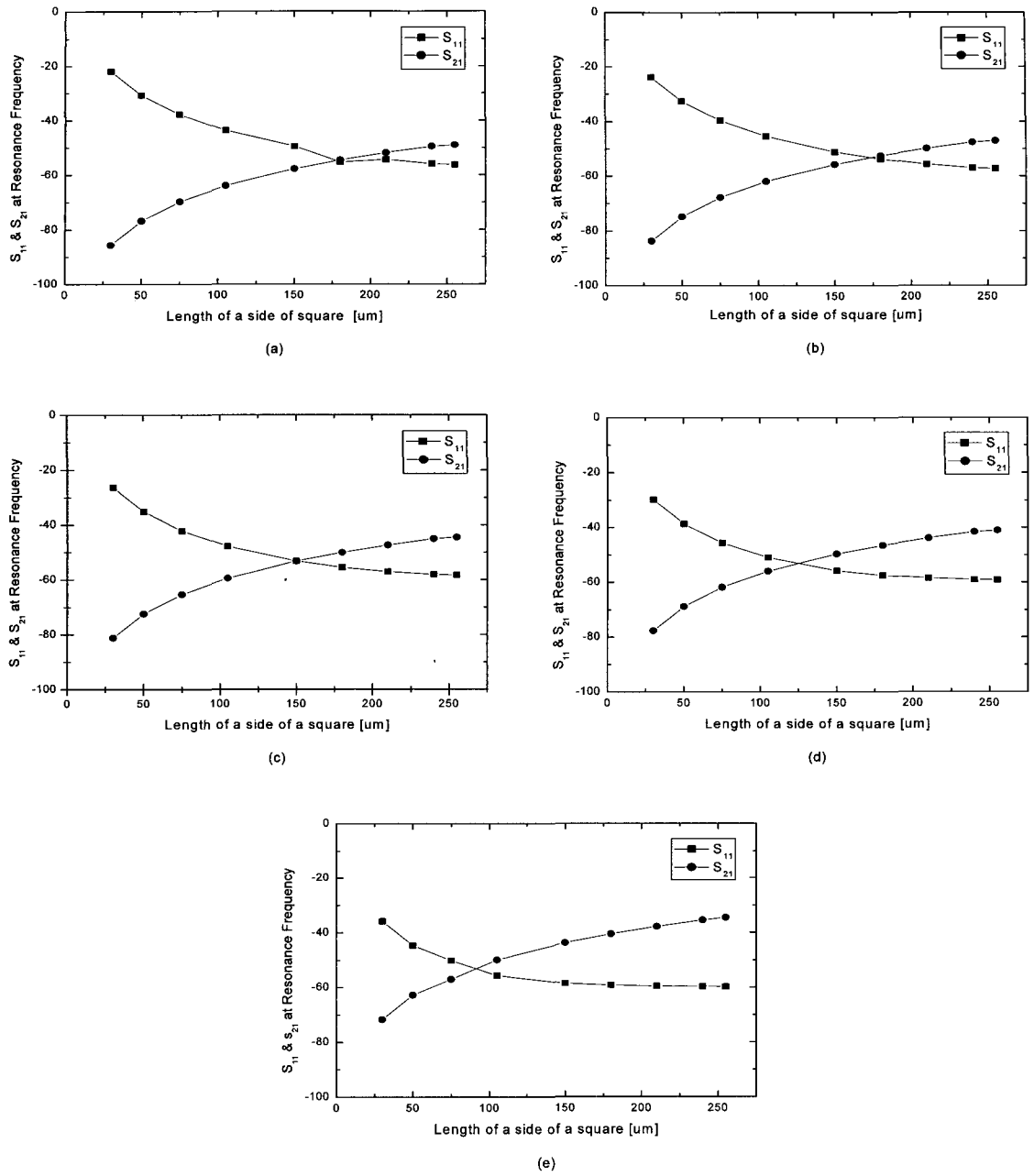

Fig. 6. S_{11} and S_{21} of FBARs with different area ratios; (a) 10:1, (b) 8:1, (c) 6:1, (d) 4:1, and (e) 2:1.

in 3×3 filter to 7.998 dB in 4×2 filter for the bandwidth of 24 MHz. These results were indicated that the increase of the number of shunt resonator rather than the number of series resonator causes the increase of insertion loss. Based on the above result, S-parameter simulation at 2.2 GHz ~ 3.0 GHz band was carried out while maintaining resonance area of the series resonator unchanged and reducing resonance area of the shunt resonator. The ratio of R_{area} = $Area_{(FBAR2)}$/ $Area_{(FBAR1)}$ ranged from 0.1 to 0.5 and to get S-parameters of FBAR filters with different resonance areas was performed. Table 4 shows the simulation results for 1×1 FBAR filter with the resonance area ratio, R_{area} = $Area_{(Series\ FBAR)}$/ $Area_{(Shunt\ FBAR)}$, between 0.1 and 0.5. As shown in Table 4, the insertion loss was reduced greatly and the bandwith was increased clearly when compared to those of BAR filter with unit resonance area ratio. The insertion loss was more reduced and the bandwidth was more increased for the smaller resonance area of series resonator. However, the superior out-of-band rejection property of the filter with larger resonance area was obtained. And the most superior characteristics was obtained from the filter whose ratio of rectangular shape of shunt resonator is 10:1.

Table 3. Bandwidths and insertion losses of FBAR ladder-type filters.

Ladder-type	Area [㎛×㎛]	Bandwidth [MHz]	Insertion Loss [dB]
1×1	50×50	29	3.546
	75×75	30	3.535
	105×105	31	3.535
	150×150	31	3.561
	180×180	28	3.589
	240×240	28	3.589
2×1	50×50	28	6.048
	75×75	28	6.049
	105×105	29	6.050
	150×150	30	6.051
	180×180	30	6.051
	240×240	30	6.052
2×2	50×50	28	10.902
	75×75	28	10.904
	105×105	28	10.904
	150×150	29	10.905
	180×180	29	10.906
	240×240	29	10.906
3×3	50×50	28	19.102
	75×75	28	19.104
	105×105	29	19.104
	150×150	29	19.105
	180×180	29	19.106
	240×240	29	19.106
4×2	50×50	24	7.990
	75×75	24	7.992
	105×105	25	7.994
	150×150	25	7.994
	180×180	25	7.995
	240×240	26	7.998

Table 4. Characteristics of FBAR filters with various shunt resonance areas.

Ladder-type	Resonance of area, Series resonator	Insertion loss [dB]	Bandwidth [MHz]	Out-of-band rejection [dB]
1×1	50×50 ㎛^{2}	0.037~1.034	52~53	0.045
	75×75 ㎛^{2}	0.420~1.949	37~39	3.694
	150×150 ㎛^{2}	0.433~1.955	35~37	4.321
	240×240 ㎛^{2}	0.443~1.960	26~29	8.456

3.3 Simulation results of BPF

2.4 GHz ladder-type FBAR BPFs for WLAN application were designed on the basis of the above simulation results and their characteristics was observed. Resonance area of series resonator was fixed by 240 ㎛ × 240 ㎛ and resonance area of shunt resonator was chosen to be

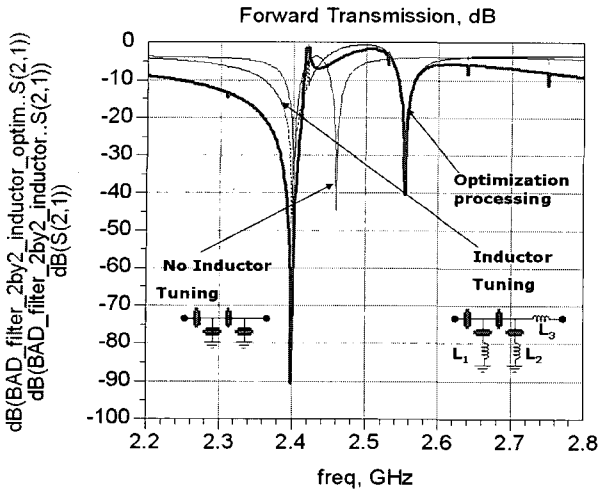

Fig. 7. Frequency response of 2×2 ladder filter.

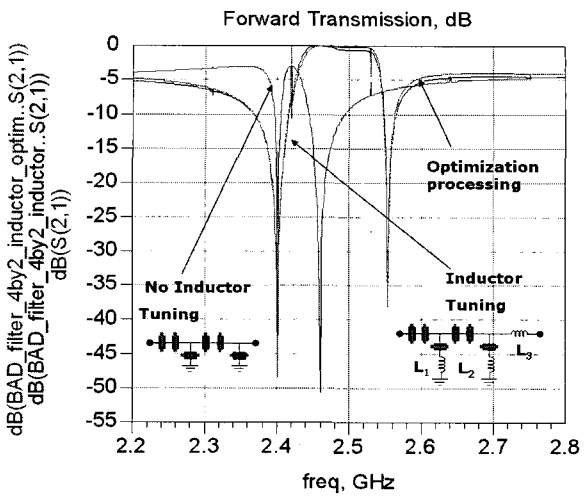

Fig. 8. Frequency response of 4×2 ladder filter.

smaller than that of series resonator. The shape of shunt resonator area was rectangular with 10:1 width to length ratio. Considering bandwidth, out-of-band rejection capability, and skirt property, the two ladder-type BPFs, 2×2 and 4×2, were adopted. Also, inductor tuning is considered due to narrow bandwidth and lower out-of-band rejection capability of piezoelectric thin-film resonator.

S-parameter simulation and inductor tuning at 2.2 GHz ~ 3.0 GHz band were performed for 2×2 and 4×2 BPFs. Using ADS program, the optimization was processed with three goals, -60 dB at 2.2~2.4 GHZ, -3 dB at 2.4~2.5 GHz, and –60 dB at 2.5~2.7 GHz. The inductor was adjusted from 0.1 nH to 10 nH for optimization process. The simulation results for 2×2 and 4×2 BPFs are presented in Fig. 7 and Fig. 8, respectively. Also, the simulation results are summarized in Table 5 and Table 6, respectively. The results showed that the insertion loss of BPF was decreased and the out-of-band rejection of BPF was increased with inductor tuning. From the results, adjusting resonance area diversely can increase insertion loss and bandwidth of BPF, and pass-band of BPF can be extended by minimizing the influence of parasitic capacitance using proper inductor tuning.

Table 5. Characteristics of 2×2 ladder-type BPF.

Condition	Insertion loss [dB]	Bandwidth [MHz]	Out-of-band rejection [dB]	Size of inductor [nH]		
				L_1	L_2	L_3
no tuning	3.717	32	4.126			
inductor tuning	0.700	102	6.085	3	4	4
optimazed inductor tuning	1.898	104	12.648	3.088	4.011	0.01

Table 6. Characteristics of 4×2 ladder-type BPF.

Condition	Insertion loss [dB]	Bandwidth [MHz]	Out-of-band rejection [dB]	Size of inductor [nH]		
				L_1	L_2	L_3
no tuning	3.079	30	3.393			
inductor tuning	0.094	106	6.090	3	4	4
optimazed inductor tuning	0.088	108	6.088	4.099	4.995	0.01

4. CONCLUSION

An air-gap type FBARs with resonance frequency of 2.401 GHz and anti-resonance frequency of 2.460 GHz were designed using Leach equivalent model to construct 2.4 GHz ladder-type BPF. Return loss (S_{11}) and insertion loss (S_{21}) of FBAR showed the opposite tendency with resonance area of FBAR increased. S_{11} was increased from 41.828 dB to 59.955 dB when the resonance area of FBAR changed from 30 ㎛×30 ㎛ to 255 ㎛×255 ㎛. The effects of numbers of series and shunt resonators on ladder-type BPF were examined by varying the number of series and shunt resonators connected. Insertion loss (S_{21}) was increased from 3.546 dB in 1×1 filter to 19.106 dB in 3×3 filter while the bandwidth remained within 28 MHz~31 MHz. S_{21} of BPF was reduced and out-of-band rejection of BPF was increased with inductor tuning. Insertion loss and bandwidth of BPF diversely can be increased by adjusting resonance area, and the influence of parasitic capacitance of BPF was minimized using proper inductor tuning, which can extend pass-band of BPF. The best characteristics were obtained when the sizes of series and shunt resonator are 150 ㎛×150 ㎛ and 5 ㎛ ×50 ㎛, respectively. In addition, out-of-band rejection was improved about 10 dB and bandwidth was broadened from about 30 MHz to about 100 MHz by inductor tuning on 2×2 and 4×2 ladder-type BPF.

ACKNOWLEDGMENT

This work was supported by the Brain Korea 21 Project in 2006.

REFERENCES

[1] "IEEE STD 802.11g/D1.1", Supplement to ANSI/ IEEE Std 802.11, 1999 Edition, 2002.

[2] R. Ruby and P. Merchant, "Micromachined thin film bulk acoustic resonators", IEEE International Frequency Control Symposium, p. 135, 1994.

[3] G. R. Kline, K. M. Lakin, and R. S. Ketcham, "Thin film resonator(TFR) low insertion loss filter", IEEE Ultrasonics Symposium, p. 339, 1988.

[4] R. S. Naik, J. J. Lutsky, and R. Rief, "Mesurements of the bulk, c-axis electromechanical coupling constants as a function of AlN film quality", IEEE Transaction Ultrasonics, Ferroelectrics, and Frequency Control, Vol. 47, No. 1, p. 292, 2000.

[5] R. Ruby, P. Bradley, J. D. Larson, and Y. Oshmyansky, "PCS 1900 MHz duplexer using thin film bulk acoustic resonator", Electronics letters, Vol. 35, No. 10, p. 794, 1999.

[6] J. D. Larson, R. Ruby, P. Bradley, and Y. Oshmyansky, "A BAW antenna duplexer for the 1900 MHz PCS Band", IEEE Ultrasonics Symposium, p. 887, 1999.

[7] L. M. Lakin, G. R. Kline, and K. T. Macarron, "High-Q microwave acoustic resonators and filter", IEEE transactions on Microwave Theory and Techniques, Vol. 41, No. 12, p. 2139, 1993.

[8] W. P. Mason, "Electromechanical Transducers and Wave Filters", D. Van Nostrand, New York, 1942.

[9] W. P. Mason, "Physical Acoustic Principles and Methods", Academic press, Newyork, 1964.

[10] W. M. Leach Jr., "Controlled-source analogous circuits and SPICE models for piezoelectric transducers", IEEE Trans UFFC, Vol. 41, p. 60, 1994.

[11] S. V. Krishnaswamy, S. S. Horwitz, and R. A. Moore, "Microwave film bulk acoustic resonator and manifold filter bank", U.S. Patent 5 185 589, 1993.